Indium-doped GaAs: Investigation of deep traps

J. P. Laurenti,* K. Wolter, P. Roentgen, K. Seibert, and H. Kurz
Institute of Semiconductor Electronics, Aachen Technical University, D-5100 Aachen, Federal Republic of Germany

J. Camassel
Groupe d'Etude des Semiconducteurs, Institut de Recherche sur les Matériaux pour l'Electronique, Université des Sciences et Techniques du Languedoc, F-34060 Montpellier CEDEX, France
(Received 27 July 1988; revised manuscript received 21 November 1988)

The effect of indium incorporation on the concentration of deep traps in a series of GaAs epitaxial layers has been investigated by performing quantitative photoluminescence (PL) and capacitance [deep-level transient spectroscopy (DLTS)] spectroscopic studies. All samples were epitaxial layers of *n*-type GaAs:In, grown by organometallic vapor-phase epitaxy (OMVPE) on liquid-encapsulated Czochralski (LEC) -grown GaAs:Cr substrates. The calibrated indium concentration ranged between 0 and 6.5×10^{19} atoms cm^{-3}, which is about 0.3% in alloy composition. We have investigated (i) the bands associated with chromium in both the epitaxial layers and the original substrates; (ii) a large recombination band, associated with an unidentified (D-V_{Ga}) complex, at about 1.2 eV; and (iii) the DLTS signal associated with the well-known deep trap *EL2*. We find the following. First, there is a one-to-one correspondence between the PL intensity associated with Cr^{2+}, at 0.84 eV, and the D-V_{Ga} signal at 1.2 eV. This is true for both the epitaxial layers and the original substrates and suggests identification of the unknown donor participating in the D-V_{Ga} complex as Cr^{4+}. Second, we find all PL intensities to decrease with increasing indium concentration, while the concentration and depth profile of *EL2* are not affected. In contrast to the near-band-edge PL intensity, which increased with increasing indium content, there is a drop by about 1 order of magnitude for all chromium-related features when going from indium-free to about 0.3% indium-rich sample. Moreover, there is a one-to-one correspondence between the increase in the near-band-edge PL intensity and the decrease in the chromium-related signals. This establishes, on a fully experimental basis, the relative roles played by indium and chromium in our epitaxial samples: both compete to incorporate on gallium sites in the strain field of neighboring vacancies but, because of a higher incorporation rate, increasing the indium concentration in the gas phase, one lowers the amount of residual chromium present at those specific sites. This results in closing low-energy recombination paths and increases the near-band-edge PL efficiency.

I. INTRODUCTION

In bulk GaAs technology, indium incorporation has been reported as an efficient way for reducing dislocations density.[1,2] As a result 3-in.-diam ingots have been recently grown which contain only 100–300 dislocations/cm^2 over 80% of their diameter.[3,4] While standard semi-insulating (SI) liquid-encapsulated Czochralski (LEC) -grown GaAs wafers exhibit about 10^4–10^6 dislocations/cm^2 with a characteristic W-shaped distribution indium-doped crystals are almost dislocation free and the etch-pit density drops by several orders of magnitude. Moreover, they seem to exhibit a greater degree of hardness during polishing operations.[3] All these considerations result in significant improvements of the electrical and mechanical properties of the material used for the fabrication of SI (mostly Cr-doped) substrates[4] and lead the way for the realization of high-performance electronic and optoelectronic integrated circuits (IC). As a direct consequence, the way in which indium is incorporated in GaAs has become a field of interest for many years (see, for instance, Refs. 3–9) and a simple mechanism to explain the reduction of dislocations density has been proposed. It involves the large volume mismatch ($\approx$21%) existing between $InAs_4$ and $GaAs_4$ molecular clusters which would induce a uniform relaxation of the lattice strains. In turn this would reduce the dislocations density. This is the basic idea of the so-called solution-hardening model.[9] However, recent investigations of the change in plastic yield between undoped and indium-doped GaAs wafers[3] have shown that over a large range of temperature, no clearly discernible difference in mechanical behavior could be distinguished between both undoped and indium-doped LEC samples. This contradicts the solution-hardening model. Indeed, in this case, one would expect a substantial strengthening of the lattice due to the presence of the solute tetrahedral $InAs_4$ defects in the GaAs matrix. Moreover, this suggests that the mechanism by which indium reduces the dislocation density in bulk GaAs might be only effective at temperatures near the melting point, when pulling out the crystals, and calls for additional investigations.

In order to find reliable results, these investigations should be performed with use of epitaxial samples grown under carefully controlled conditions. However, concerning such epitaxial layers, which would correspond to

the active parts of the devices, not much attention has been paid.

The first reports concerned liquid-phase epitaxial (LPE) samples[10] in which the concentration of deep traps was investigated both by photoluminescence (PL) and capacitance [deep-level transient spectroscopy (DLTS)] techniques. In this case, a strong reduction in deep traps was found, which explained the resultant (and significant) improvements in the device characteristics already claimed.[11] More recently the growth of dislocation-free and indium-doped GaAs layers, using molecular-beam epitaxy (MBE) techniques onto a dislocation-free indium-doped GaAs substrate, has been also reported.[12] Provided that the lattice mismatch ($\Delta a_\perp / a_0$) was kept less than $\pm 4 \times 10^{-4}$, no misfit dislocations were generated but, in this case, the role of indium was not clear. Indeed, dislocation filtering and defect reduction effects are well known and have been reported between adjacent layers when there is a significant difference between their lattice constants and elastic moduli. Depending on the relative layer thicknesses, there is or not an elastic accommodation of the interlayer misfit,[13] and this is the reason for the successful growth of "free-standing" as well as "strained" superlattices. Both have been reported in the literature.

In order to master the isoelectronic doping of GaAs, and understand the microscopic mechanism of indium incorporation and defect compensation, we believe that more investigations should be done. In a first paper,[14] hereafter referred to as paper I, we investigated in great detail the influence of indium incorporation in a series of GaAs epitaxial layers grown by organometallic vapor-phase epitaxy (OMVPE). In order to insure reliable results, special care was taken to determine quantitatively the indium concentration. For the highest compositions, the lattice constants were determined by using a precision double-crystal x-ray diffractometer and the {115} reflection plane of the crystal monochromator. Then the strain-free lattice constant was calculated, assuming both the lattice matched to the substrate (this gives $\Delta a / a_{\text{substrate}} = 0$) and a Poisson ratio of 0.29. Finally, by simply applying Vegard's law, the In concentrations could be calculated. Since, for low-In concentrations, the respective x-ray diffraction peaks associated with the substrate and the epilayer could not be resolved, quantitative secondary-ion mass spectroscopy (SIMS) measurements have been performed. This was next generalized to determine the relative In concentrations in the different layers, and the ratio of In counts, normalized to the As matrix signal, was systematically determined. A comparison between the absolute x-ray determination and the relative SIMS data showed good agreement on the samples with the highest-indium concentrations and the combination of both techniques ensured reliable values from 0.03 to 0.29 at. % in indium composition (see Table I).

The results obtained concerned the change in band-gap energy, the concentration of residual impurities and the low-temperature (2 K) photoluminescence (PL) efficiency. We have found the following.

(i) Even at very low concentration, indium incorporates like a constituent of the solid solution $Ga_{1-x}In_xAs$. We could not find any evidence of clustering between neighboring isoelectronic substituents (like nitrogen atoms incorporating into gallium phosphide,[15] for instance) or detect any disorder-enhanced polariton recombination lines.[16] This makes indium-doped gallium arsenide a prototype dilute alloy system.

(ii) Quantitatively analyzing the shift of the luminescence lines versus indium composition, we could find small but significant differences between the slope parameters corresponding to the substitutional impurities Zn or Mg, on the one hand, and C, on the other hand. This is well accounted for by a simple cluster model of 17 atoms which discerns between impurities substituted on the cationic (Zn,Mg) or the anionic (C) sites, respectively.

(iii) Quantitatively analyzing the change in PL intensity versus indium concentration, we could establish a rather drastic increase. This indicates an improvement in the near-band-edge optical quality of the sample which saturates near 2×10^{19} indium/cm^3 (about 0.1% molar concentration).

In the present work, we report on a series of quantitative investigations related with the concentration of deep traps in the same series of GaAs:In samples. Since we are mainly interested in the discussion of fundamental problems encountered in the course of GaAs-IC technology, we focus on the following.

(i) First, we examine the concentration of chromium migrating from the substrate to the epitaxial layers. We find a decrease with increasing indium content, by about

TABLE I. Sequence of growth runs, Hall measurement data, and indium concentrations [In] in GaAs:In OMVPE layers, as determined by x-ray diffraction and quantitiative SIMS measurements. The [In] values in % are listed with respect to GaAs molecular concentration. In the last column, estimated upper error limits are also displayed.

Growth run	$N_D - N_A$ (10^{15} cm^{-3})	Mobility (Hall meas.) ($cm^2 V^{-1} s^{-1}$) 300 K	77 K	[In] (x-ray diffraction) (10^{19} cm^{-3})	(%)	$^{113}In/^{75}As$ SIMS counts	[In] (combination of x-ray and SIMS data) (10^{19} cm^{-3})	(%)
1	4.5	4350	22 330	dummy layer				
6	0.9	7066	51 060	In-free GaAs				
5	0.8	7097	51 160	not resolved		193	0.7	0.03±0.01
4	0.5	7323	17 555	(0.9)	(0.04)	320	1.1	0.05±0.01
2	1.3	6778	38 520	1.90	0.086	530	1.90	0.086±0.005
3	1.3	7145		6.34	0.287	1780	6.41	0.290±0.005

one order of magnitude, of the PL signal associated with the Cr^{2+} zero-phonon line (ZPL) at energy 0.84 eV.

(ii) We focus on the concentration of gallium vacancies. This was done by inspecting the changes which affect a large PL band at 1.2 eV. It is related to a series of $(D\text{-}V_{Ga})$ complexes and we have found that, in our case, the unknown donor was Cr^{4+} and the concentration in gallium vacancies independent of the indium composition.

(iii) We examine the concentration of $EL2$. A definitive (and well-accepted) identification of $EL2$ is still lacking but all experimental data indicate that $EL2$ is a complex defect which starts from an As_{Ga} antisite. The identification of the other partner is not so clear (it could even be a "family" of $EL2$ defects[4]) but recent experimental results[17] suggest a second-nearest-neighbor arsenic interstitial in the $\langle 111 \rangle$ direction. In this case, the increase in $EL2$ concentration around dislocations would simply correlate with the arsenic precipitates which decorate the dislocations. Such precipitates, providing enough arsenic atoms to fill the gallium vacancies, would result in the simple equation

$$2\ As_i + V_{Ga} \rightarrow As_{Ga} + As_i\ (EL2)\ . \quad (1)$$

We have used DLTS measurements to probe the concentration and depth profile of $EL2$ but could not find any significant effect of the indium incorporation on this dominant electron trap.

II. EXPERIMENTS

All details concerning the sample preparation have been given in paper I and will not be repeated here. However, for the sake of completeness, a summary of the various parameters which characterize our epitaxial series of samples is given in Table I.

Our PL measurements have been done with the samples held at 2 K in a liquid-helium bath. The 647.1-nm line of a Kr^+ laser was used as exciting frequency with a power density of 44 W/cm^2 and, depending on the range of wavelength investigated, the PL signal was detected using different photodetector systems. First, in the range $h\nu > 0.7$ eV a Ge detector, cooled down to liquid-nitrogen temperature, was used. This resulted in all PL spectra displayed in this work. Next, in the range $h\nu < 0.7$ eV, a Peltier-refrigerated PbS cell was used. However, despite intensive searchs, no significant PL signal could be found in this energy range. In both cases, conventional lock-in detection techniques and numerical data-storage and acquisition systems were used. The experimental resolution was typically 0.5 meV at about 1 eV and we used a 0.5 m grating monochromator.

To perform DLTS measurements a series of Schottky diodes were fabricated in the following way. After defining a 1000-μm-diam mesa, a first series of two semicircular Ni/Au-Ge/Ni Ohmic contacts were evaporated and alloyed at 460 °C for 1 min in a nitrogen flow. This defined a ring in the center of which a small dot of 600 μm diameter was next evaporated to form a Ti/Pt/Au Schottky contact. Finally, the whole system was connected and a series of I-V characteristics for all diodes was recorded. In the reverse direction, typical leakage current densities of 10^{-6} A/cm^2 up to -60 V have been found while, in the forward direction, the ideality factors improved from 1.25 to 1.01 with increasing indium concentration. This is in agreement with typical results previously reported.[10]

From our C-V measurements, we determined both the carrier profiles and the heights of various titanium/n-type GaAs Schottky barriers. All results have been summarized in Table II. We find (i) a flat carrier profile; (ii) free-electron concentrations in close agreement with the Hall concentrations (also listed in Table II); and (iii) diffusion voltages in the range 0.8–0.9 eV, as expected for standard Ti-GaAs (n-type) Schottky contacts.

Our DLTS system has been already described in Ref. 18. The samples were mounted in a cryostat which operates in a helium gas flow. By combining both the entrance of the cold gas and an additional thermal flux (by electrical heating), one could sweep the temperature from 4.6 to 370 K. At selected values of the temperature, a series of capacitance transients (1000 values) was stored using a microcomputer but, instead of the total capacitance, the capacitance bridge amplifies capacitance varia-

TABLE II. Indium concentrations [In], free-electron concentrations, and diffusion voltages of Ti n-type GaAs: In Schottky diodes for each In-free GaAs and GaAs:In OMVPE layer. The [In] values in % are listed with respect to GaAs molecular concentration. When two different values are given for the same sample they correspond to different diodes achieved on the same sample.

	[In] concentration (10^{19} cm^{-3})	(%)	Free-electron concentration at 300 K (10^{15} cm^{-3}) Hall data	C-V plot	Diffusion voltages (V)	$EL2$ concentration (10^{16} cm^{-3})	Run number
In-free	0	0	0.92	1.3	0.81	2.5	6
GaAs				1.5	0.84	2.2	
GaAs:In	0.7	0.03	0.82	1.4	0.81	2.3	5
				1.0	0.81	2.6	
	1.1	0.05	0.45	0.6	0.79	3	4
	1.90	0.086	1.3	1.2	0.87	3	2
				1.4	0.88	2.1	
	6.41	0.29	1.3	1.8	0.79	2	3
				1.8	0.78	1.9	

tions $dC(t)$ in a specific frequency range. The capacitance resolution obtained in this way is about 0.09 fF and such a sensitivity enables one to determine concentration depth profile of deep centers with a 10 nm resolution. This is close to the Debye length and requires performing precise differential analyses of the experimental transients. In our case, this was done by fitting an exponential function with the recorded data. This method improves the accuracy in the determination of trap signatures (thermal activation energy $E_C - E_T$ and capture cross section σ) with respect to the conventional boxcar technique by a factor of 10^3.

III. PL RESULTS

Since the use of SI substrates considerably simplifies the design and reduces the cost of integrated-circuit (IC) technology, we have mainly investigated, in our OMVPE-grown GaAs layers, the concentration of chromium atoms which migrate from the substrate and incorporate in the epitaxial layers. We report also on the 1.23-eV PL band which is indicative of a $(D\text{-}V_{Ga})$ complex. Lastly we have checked for a PL signal associated with $EL2$ (which would tell us about As antisites) but could not find any.

A. Chromium level in GaAs:In

Chromium in GaAs is a prototype transition-metal impurity. It substitutes preferentially for gallium and, in the neutral configuration, is given the ionic notation Cr^{3+}. When it receives an extra electron in the $3d$ shell, it behaves like a simple acceptor and is designated as Cr^{2+}. Two different series of Cr^{2+} centers have been identified and have been designated as Cr^{2+}(I) and Cr^{2+}(II). They differ in two ways: first by the local site symmetry (tetragonal and trigonal, respectively) and second by the corresponding energy of the internal transitions $5E \rightarrow 5T_2$ (0.82 and 0.84 eV, respectively). All details concerning chromium in GaAs can be found in a comprehensive review given by Bates and Stevens.[19]

In this work we focus on the trigonal Cr^{2+}(II) PL band which appears near 0.84 eV in Fig. 1. Concerning the origin of the trigonal distortion, it comes from an associated defect X which results in the complex $(Cr^{2+}\text{-}X)_{\langle 111\rangle}$. Again, it has been some controversy about the detailed assignment of the unknown partner X but, in bulk LEC-grown GaAs:Cr, the situation is clear. It seems now well established[20] that the associated defect is an isolated arsenic vacancy (V_{As}) in the first-neighbor position. Due to the local field of C_{3v} point-group symmetry, a considerable fine structure appears[21] which is associated with the zero-phonon line at 0.839 eV (ZPL) but is not resolved in this work. The only lines found are a series of broad satellite structures which correspond to a TA replica ($\sim$0.83 eV) and several other modes at lower energy. Concerning now codoped GaAs:Cr-I, where I is a second species which can substitute either on the gallium sites (indium, silicon, tin) or the arsenic sites (sulfur, selenium, tellurium), various perturbations have been reported.[22,23] They depend on the magnitude of the additional lattice distortion. For instance two lines, labeled A and B in the work of Ref. 23 have been assigned to In-Cr related ZPL lines. They should appear at 0.873 and 0.854 eV, respectively, and their relative intensities, with respect to the standard ZPL line, will depend on the probability of finding *both* a chromium and an indium atom in the first-neighbor positions with respect to the central arsenic vacancy. They were not resolved in this work and we shall focus only on the standard features.

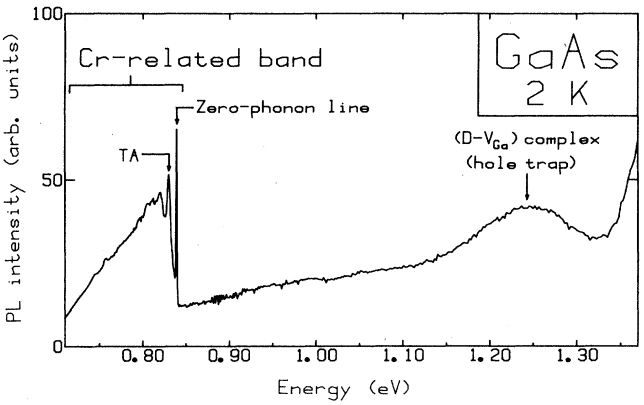

FIG. 1. Photoluminescence spectrum observed at 2 K in the range 0.7–1.4 eV. This result corresponds to the indium-free OMVPE GaAs reference sample and was corrected for the relative response of our germanium detector.

A point should be made clear first. Concerning the origin of the chromium-related features, we emphasize that the presence of chromium in our epitaxial layers does not come from any intentional doping. It comes from an outdiffusion of this element from the substrate during the growth sequence. For bulk GaAs, it is well known that the apparent chromium redistribution depends on the As partial pressure. Indeed, various results have been reported which range from an increase in Cr concentration near the surface to a strong decrease (the Cr concentration tending to zero at the surface) when the arsine partial pressure equals zero.[24] Very similar, but somewhat less documented, data have also been presented for iron in $Ga_{0.47}In_{0.53}As$ epitaxial layers grown onto InP:Fe substrates.[25] We emphasize that in this work all parameters associated with the growth sequence, i.e., the duration (30 min), the temperature of the GaAs substrate (640 °C), the arsine partial pressure (4×10^{-3} bar), the $[A^{V}]/[B^{III}]$ ratio (equal to 10), and the total pressure (1 bar) were kept constant in order to get meaningful data. Moreover, in order to approach quantitatively the effect of indium incorporation, we have taken into account the inhomogeneities of the contamination source. As a consequence, we have performed a series of routine checks by systematically analyzing the chromium-related PL bands of each piece of substrate material. The results are shown in Fig. 2(a) and reveal discrepancies in absolute intensities up to a factor of 4. We emphasize that care was taken to minimize such inhomogeneities and, before epitaxy, each substrate was cut from about the same distance relative to the slice center.[14] This points out the existence of large and unexpected inhomo-

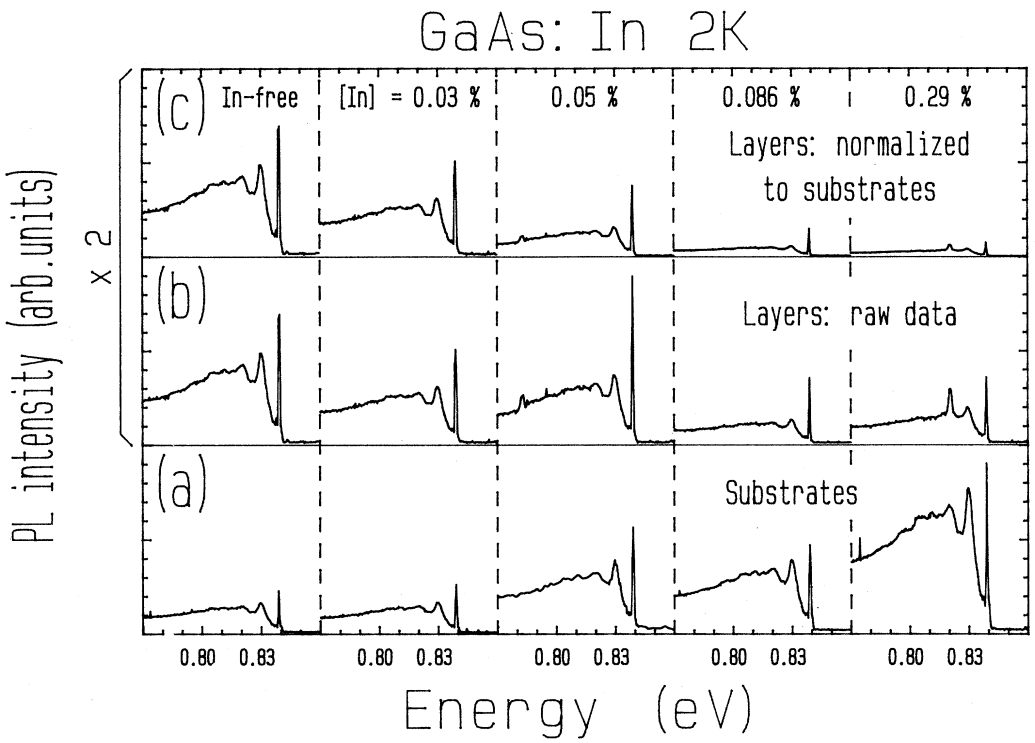

FIG. 2. Cr^{2+}-related PL bands as obtained for (a) the different substrates and (b) the respective epitaxial layers. (c) Data normalized to the substrate efficiency, showing a decrease by a factor of 10 which is illustrated in Fig. 3.

geneities in commonly used LEC-grown ingots compensated with chromium and currently available in the industry.

Figure 2(b) gives raw PL spectra for the different series of samples, while Fig. 2(c) gives normalized data. We find a clear and regular *decrease* in the PL intensity which is illustrated in Fig. 3 and saturates above about 0.1% indium composition. This relative change concerns all Cr-related PL features, including both the ZPL and TA replica or the $(D\text{-}V_{Ga})$ complex which will be discussed in the next section. It should be compared with the increase in near-band-edge (NBE) intensity which was reported in paper I. A fast *increase* was found which also saturated above 0.1% indium concentration. Since we work under constant excitation intensity, closing one recombination path should increase the number of carriers passing through the next one. In this case, one expects a one-to-one correspondence between the PL intensity associated with the near-band-edge optical features D^0X, A^0X, and $(DA)_c$ recombination lines, on the one hand, and the chromium-related features, on the other hand. This has been checked for both the zero-phonon and the TA-phonon-assisted emission lines and, for clarity, is displayed in Fig. 4 for the ZPL only. Obviously we find a strong inverse correspondence, the NBE optical features being higher (lower) the lower (higher) is the ZPL signal whatever the indium composition may be. The full line is a least-mean-square fit through the experimental data which gives

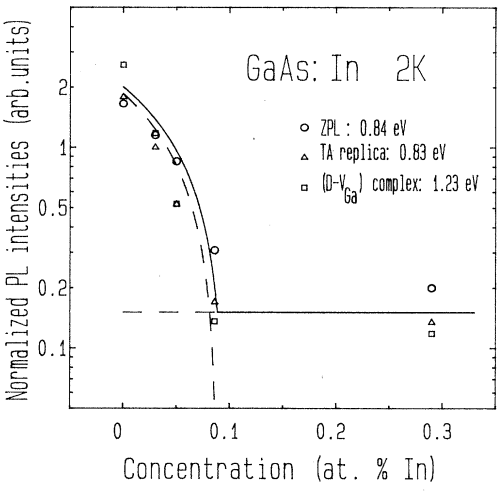

FIG. 3. Relative changes in chromium-related PL bands vs indium concentration. The relative intensities have been normalized in such a way that the ratio is one when the same PL intensity comes from both the epitaxial layer and the corresponding piece of substrate. The connection of the 1.23-eV emission band with chromium concentration is discussed in the text. In solid line is a simple prediction as discussed in the text. The dashed lines illustrate the two contributions: a constant background in the range $n_i > 10^{-3}$ at. %, and a strongly composition-dependent contribution in the range $n_i < 10^{-3}$ at. %.

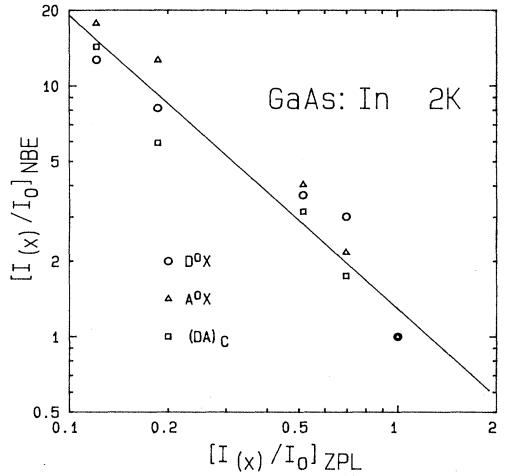

FIG. 4. Inverse scaling law observed for the relative intensity of the near–band-edge transitions vs chromium-related features (log-log scale). The NBE optical signals are higher (lower) the higher (lower) the indium concentration. The solid line is a least-mean-square fit as discussed in the text.

$$(I_{(x)}/I_0)_{\mathrm{NBE}}=1.29/[(I_{(x)}/I_0)_{\mathrm{ZPL}}]^{1.17}\ , \tag{2}$$

where I_0 corresponds to our In-free reference layer. As expected, we find almost exactly an inverse correspondence and, from this simple relationship, we show the following points.

(i) Most of the NBE optical properties of our indium-doped GaAs epitaxial samples are ruled by an interplay of chromium *and* indium, both incorporating on gallium sites.

(ii) Chromium, in order to explain the prefactor 1.29, not only participates in the Cr_{Ga}-X complex as an acceptor Cr^{2+} but *does* also participate in more complex defects. We shall come back to this point in the next section.

B. (D-V_{Ga}) complex

This corresponds to the large luminescence band found around 1.23 eV (see Fig. 1). Few investigations have been conducted in this energy range and the more reliable ones have been done by Williams.[26] They concern a series of gallium vacancy-donor substitutional complexes, the so-called (D-V_{Ga}) complexes. Depending on the donor species, and the lattice sites where they substitute, the peak energy varies. However, whatever the donor species, the residual concentration (N_d-N_a) must be in the range $10^{16}-10^{18}$ cm^{-3} in order to get a clear PL signal. This has been confirmed in successive works[27] and is, at least, 1 order of magnitude above the residual donor concentration achieved in this work. This makes the residual amount of Se atoms present in our epitaxial layers (see paper I) to be hardly involved in the origin of the strongly luminescent band experimentally found at 1.23 eV.

Moreover, when checking the luminescence of the different pieces of substrates, we have found the same luminescence band to be already present in the raw material. It varies from sample to sample, but in both the substrates and the epitaxial layers, we find a one-to-one correspondence with the intensity of the Cr-related PL band at 0.83–0.84 eV. This is shown in Fig. 5, where the various triangles (dots) refer to various pieces of layers (substrates), respectively, and all luminescence intensities concern raw data. As a consequence, we believe that the 1.23-eV luminescence band, in our chromium-doped samples, comes from a complex of the type (D-V_{Ga}) in which the donor partner is a Cr^{4+} stabilized by the neighboring gallium vacancy. Evidences of amphoteric behavior for the substitutional impurity Cr_{Ga} in GaAs have long been given in p-type material[28] but, as far as we know, this is the first report of a Cr^{4+} behavior in n-type material. Up to now the identification of isolated Cr^{4+} as a compensating center was given only in p-type material[29,30] but never reported in n-type samples. This is because, lying 324 meV above the valence band, it can only act to compensate shallow (residual) acceptors and does not participate in the population of the conduction band. When joined with a neighboring gallium vacancy, which is assumed to act as an ionized acceptor, the system relaxes and becomes stable in an energetic configuration close to the standard (D-V_{Ga}) complexes, where D is more usually Si, Sn, S, Se, or Te. Similar data have been reported for the deep-donor carbon:[31] while it is not found in the usual way, it was reported to participate also in a (C_{Ga}-V_{Ga}) complex.[26] Since it seems now well established that in GaAs very little carbon goes isolated on the gallium site, this would indicate that selective incorporation effects appeared which can be driven by the presence of a cationic vacancy.

Normalizing the PL intensity for the different epitaxial layers with the corresponding PL intensity of the substrate, we get again a decrease by a factor of 10 versus in-

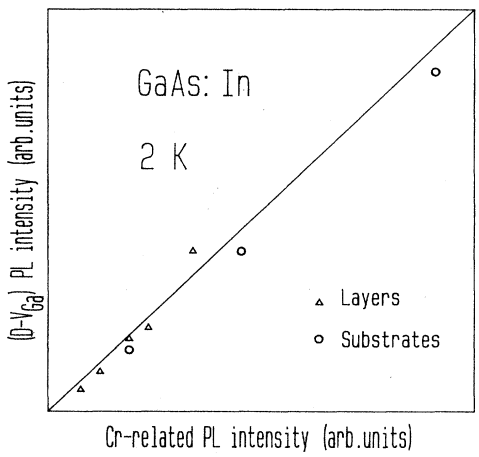

FIG. 5. Intensity of the PL signal associated with the unidentified (D-V_{Ga}) complex plotted against the intensity of the Cr^{2+} related PL intensity. The triangles (dots) refer to various epitaxial layers (substrates), respectively. The good correlation obtained demonstrates that again chromium participates in the definition of the (D-V_{Ga}) complex.

dium content. This was already shown in Fig. 3, where all data given for the (Cr^{4+}-V_{Ga}) complex closely correlate with the features of the (Cr^{2+}-V_{As}) complex. Since both series of anionic and cationic vacancies are independently involved together with chromium, this demonstrates (i) that there is no quantitative change in the concentrations of gallium and/or arsenic vacancies versus indium content, (ii) that there is only an interplay of indium and chromium to incorporate in the strainfield of the neighboring defect. At low indium composition, when chromium incorporates easily, we find strong luminescence signals which are the "signatures" of the two chromium-related centers. Now, increasing the indium concentration, we find that chromium does not incorporate so easily and the PL signal start to decrease. In any case the concentration of V_{As} and V_{Ga} is not affected.

C. Search for *EL*2-related PL band

In bulk GaAs, *EL*2 is a deep center which has the ability to compensate the material. This has been widely demonstrated[32,33] and constitutes now a current technique in growing SI crystals used as substrates in IC technology.[4] On the microscopic scale, it is associated with As_{Ga} antisite defects complexed with a (or a series of) unknown partner(s)[33] and acts as a deep donor which compensates shallow residual (mainly zinc or carbon) acceptors. In this state it becomes *EL*2(+). In *p*-type material, a luminescence band at 0.68 eV has been reported[32] which corresponds to the following scheme:

$$EL2(+)+e^{-}(\mathrm{CB})\rightarrow EL2(0)\ , \tag{3a}$$

$$EL2(0)+h^{+}(\mathrm{VB})\rightarrow EL2(+)+h\nu\ (\mathrm{photon})\ . \tag{3b}$$

In *n*-type materials compensated with chromium, no simultaneous investigation of Cr and *EL*2 has ever been given. On the one hand, the insulating properties of the material preclude the use of electrical (DLTS) measurements and, on the other hand, no optical report of *EL*2 exists. As a matter of fact, in our substrate material which is *n*-type (slightly As-rich) and Cr-compensated, we have checked if, using only above-band-edge excitation, we could find any luminescence signal associated with *EL*2(0). This attempt was unsuccessful. All photogenerated carriers were recombined before coming into the vicinity of the neutral trap and only intracenter (below band edge) excitation would be efficient.[32] This was not attempted here.

Concerning our epitaxial layers, the average chromium compensation was smaller and we could now perform DLTS investigations. The results will be given in the next section. However, on the optical side, we could still not resolve any luminescent signal associated with *EL*2(0). This is interesting to notice since the DLTS data confirm that there is no incompatibility between the two different species of deep centers. This would be the case, for instance, if one supposed that, because of an increase of the presence of substitutional chromium on the gallium site, the concentration of gallium vacancies and/or arsenic antisites would reduce. In the preceeding section we have seen that this is just not true for the gallium and/or arsenic vacancies. We shall see the same for the arsenic antisites in the next section. As a matter of fact, this discrepancy comes only from the charge state of *EL*2. In *p*-type material, where *EL*2 is an ionized donor which compensates a shallow acceptor, a clear PL band can be observed even using above-band-edge excitation. On the other hand, in the *n*-type material where *EL*2 is in a neutral state and cannot contribute to an efficient radiative recombination path, it is mainly detected by DLTS technique. This was the case of the samples investigated here.

IV. DLTS MEASUREMENTS

Current data indicate that, in GaAs grown by OMVPE, *EL*2 is a dominant electron trap.[34] This was the case of our indium-doped samples. We display typical DLTS spectra in Fig. 6 and, obviously, only one single-electron trap can be found. From the Arrhenius diagram plotted in Fig. 7 for our pure GaAs sample, we find a thermal activation energy $E_C-E_T=0.79$ eV and a capture cross section $\sigma=5.6\times10^{14}$ cm^2.

This is in rather good agreement with previous results[35] and no significant change in these parameters could be detected as a function of indium concentration. As illustrated in Fig. 6, for the same time window but different indium concentrations, the magnitude of the DLTS peaks associated with *EL*2 scatter by about 46% but no monotonic change associated with the incorporation of indium could be found. This behavior strongly departs from the monotonic decrease of the Cr- and (D-V_{Ga})-related PL intensities already noticed (see Sec. III) but, comparing different diodes realized on the same sample (see Table II), we notice an average discrepancy of the DLTS signal by about 26% for a given layer. Therefore we feel that the maximum scattering amplitude of 46% noted in Fig. 6 is only weakly related to the change in indium concentration but mostly comes from a lack of reproductivity from diode to diode and sample to sample. As a consequence, we concluded that our DLTS data do not show a clear decrease in the *EL*2 concentration versus indium incorporation in our OMVPE samples.

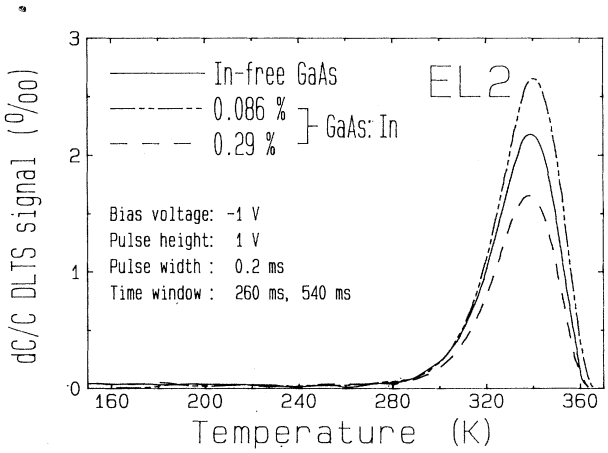

FIG. 6. DLTS spectra of both the reference *n*-type In-free GaAs sample and two GaAs:In OMVPE layers, recorded with the same time window.

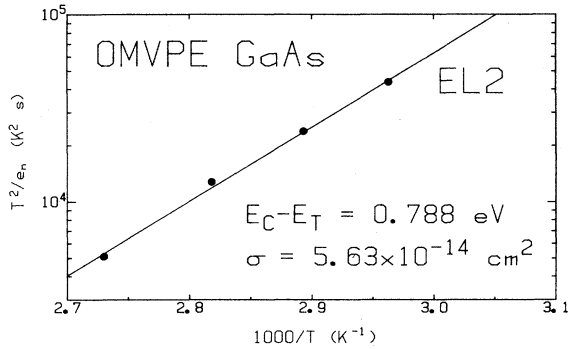

FIG. 7. Arrhenius diagram of $EL2$ electronic trap in an n-type GaAs OMVPE layer.

This is in agreement with the report of Ref. 6.

Precise depth profiles for the $EL2$ density have been also determined for every epitaxial layer by changing the bias voltage and the filling pulse height. They are shown in Fig. 8 for the In-free reference sample and for one sample of GaAs:In. Taking into account the growth temperature (640 °C), the mole ratio (equal to 10), and the unintentional doping we find a rather flat profile with an average $EL2$ concentration close to 2×10^{14} cm^{-3}. This is again in good agreement with previous data.[34] A tendency for the $EL2$ density to increase seems to occur when the surface is approached. This is also in agreement with Ref. 34. This profile, as well as the average $EL2$ density, remains the same for all indium concentrations and confirms the noninfluence of indium incorporation on this dominant electron trap in our investigated series of OMVPE layers.

V. GENERAL DISCUSSION

Investigating the effect of indium incorporation on both the NBE intensity (paper I) and the deep-trap content (this work), we have found that most experimental results could be accounted for by an interplay of indium and chromium, incorporating at specific sites, in our epitaxial samples. Since there was no intentional chromium doping this suggests that, *during the growth,* the incorporation of chromium atoms out diffusing from the substrate is controlled by the amount of indium atoms present in the material and/or the gas phase. This does not tell us anything about the details of the mechanism. To shed more light on this point, we have performed an investigation of the chromium distribution in two continuously etched samples. The corresponding data can be found in Fig. 9. One sample, which is indium free, was our dummy layer. It shows an accumulation of chromium in the bulk of the epitaxial layer [see Fig. 9(a)]. This is clear from a consideration of both the ZPL (open circles) and the TA replica (triangles): in both cases, the maximum PL amplitude appears after etching about 5000 Å of the epitaxial layer. The apparent profile is Gaussian, with a rather constant contribution coming from the bulk of the material. Both solid lines are simple theoretical fits assuming first, a standard diffusion mechanism through the interface,

$$C_i(x)=C\left[1\pm\mathrm{erf}\left[\frac{|x-x_i|}{2L_D}\right]\right], \tag{4a}$$

and, second, a Gaussian distribution which appears only because of an incorporation mechanism through the gas phase,

$$C_0(x)=C'\exp\left[-\left[\frac{x-x_0}{2L_D'}\right]^2\right]. \tag{4b}$$

Here, x_i and x_0 refer to the interface and the center of the Gaussian distribution, respectively. $L_D=(Dt)^{1/2}$ is the diffusion length for chromium; D is the diffusion constant, and t the growth duration, 30 min for all our epitaxial layers. At last, the length L_D' is the standard deviation in the Gaussian distribution. Using the numerical data listed in Table III, such an incorporation mechanism fits very well with the experimental data. The values $D=4\times10^{-12}$ cm^{2}s^{-1} and $L_D=0.85$ μm, used for the standard diffusion process through the interface, are typical for the diffusion of chromium in GaAs.[23] The standard deviation $L_D'=1.20$ μm in the Gaussian distribution is close to the diffusion length. Of course this departs

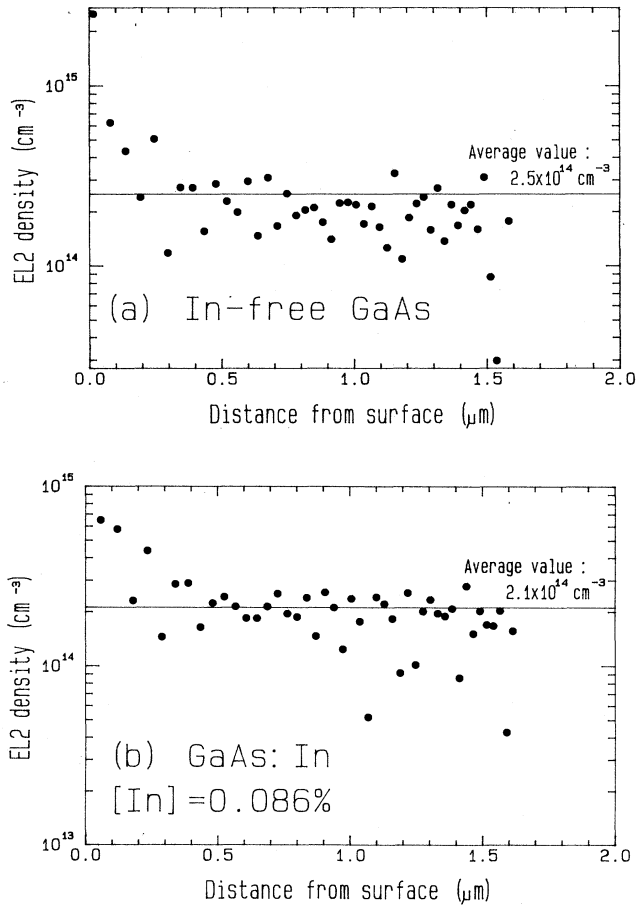

FIG. 8. Depth profile of $EL2$ density obtained in our n-type OMVPE layers. (a) In-free GaAs (reference sample), (b) GaAs:In (the indium concentration was 0.086%).

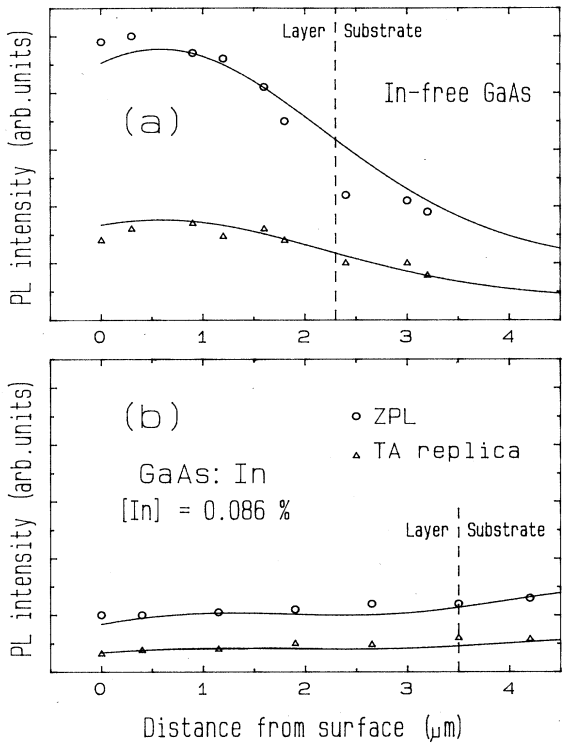

FIG. 9. Depth profile of the Cr-related features. (a) In-free GaAs (dummy layer), (b) GaAs:In (the indium concentration is again 0.086%). All solid lines are theoretical fits as discussed in the text.

from usual mechanisms but demonstrates that apart from the well-known diffusion through the interface, there is indeed an effect of chromium incorporation through the gas phase (autodoping phenomenon) which (in our case) saturated at about 5000 Å from the surface. Of course, because of the very low vapor pressure of chromium at $T_g = 640\,^{\circ}\mathrm{C}$, there has to be some complexing with a decomposition product of the reaction in order to insure (i) a transportation to the surface and (ii) an incorporation to the gallium sites. This incorporation is very indium sensitive: This is clear from consideration of Fig. 9(b). The solid lines are again theoretical fits with almost identical series of parameters, except the ratio C'/C which has been lowered by one order of magnitude (Table III). The point is now that because of a higher incorporation rate of indium the surface incorporation closes up and this results in a more standard diffusion profile with a maximum value in the bulk of the source material. We believe that this is the main source of indium-related effects in our epitaxial samples.

Concerning the specific effect of indium on complex defects, which involve the association of impurities with vacancies or antisites, we find a behavior which *depends on the defect investigated*: Both concentrations of $(\mathrm{Cr}\text{-}V_{\mathrm{As}})$ and $(\mathrm{Cr}\text{-}V_{\mathrm{Ga}})$ exhibit a drastic decrease versus indium concentration while $EL2$ appears mainly insensitive. On the microscopic scale, this clearly evidences selective incorporation mechanisms during the growth sequence (indium does not incorporate as efficiently to suppress arsenic antisites as it does to substitute for chromium on the gallium sites) and can be supported by more quantitative arguments.

Let us call N_c the total concentration in cationic sites. for any given indium composition, one can write

$$N_c = [\mathrm{Ga}]_{\mathrm{Ga}} + [\mathrm{In}]_{\mathrm{Ga}} + N_{\mathrm{DCS}} , \tag{5}$$

where N_{DCS} means the concentration of "any remaining (defect) cationic site." Since we are mainly interested in this part in the concentration of arsenic antisites as a probe of $EL2$, one can write

$$\Delta[\mathrm{As}]_{\mathrm{Ga}} = -\Delta[\mathrm{In}]_{\mathrm{Ga}} - \Delta[\mathrm{Ga}]_{\mathrm{Ga}} \tag{6}$$

which shows that, increasing the indium composition, all changes in arsenic antisites come from an *increase* of the substituted $(\mathrm{In})_{\mathrm{Ga}}$ sites which is not balanced by a *decrease* of the normal $(\mathrm{Ga})_{\mathrm{Ga}}$ sites. In first order one can write

$$\Delta[\mathrm{As}]_{\mathrm{Ga}} = -\frac{[\mathrm{As}]_{\mathrm{Ga}}}{N_c - [\mathrm{In}]_{\mathrm{Ga}}} \Delta[\mathrm{In}]_{\mathrm{Ga}} \tag{7}$$

which after straightforward integration, gives versus the indium composition n_i

$$[\mathrm{As}]_{\mathrm{Ga}} = [\mathrm{As}]^0_{\mathrm{Ga}} (1 - n_i) . \tag{8}$$

This is shown as a straight line Fig. 10 and, taking account of both the range of composition investigated and the experimental uncertainty, does not correspond to any sizable effect. The key point in this section is that we made no difference between an indium atom incorporation on a "normal" $(\mathrm{Ga})_{\mathrm{Ga}}$ or a defective $(\mathrm{As})_{\mathrm{Ga}}$ cationic site. This is no longer true when dealing with chromium.

TABLE III. Numerical values of the parameters used to describe the Cr-related PL intensity profiles of Fig. 9 by Eqs. (4).

	Standard diffusion process		Incorporation through gas phase (Gaussian distribution)		
	Diffusion coefficient (10^{12} cm^2 s^{-1}) D	Diffusion Length (μm) L_D	Standard deviation (μm) L'_D	Depth of center (μm) x_0	C'/C ratio
In-free GaAs	4	0.85	1.20	0.5	9.5
GaAs:In [In]=0.086%	4	0.85	1.20	1.0	0.8

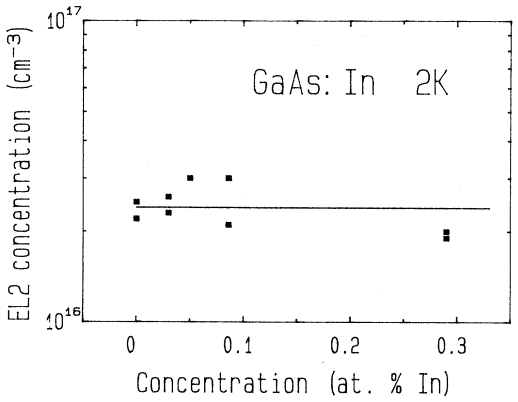

FIG. 10. Composition dependence of the *EL*2 average concentration. Solid line, a theoretical prediction assuming that there is no specific probability of incorporation for an indium atom on an arsenic antisite.

To make this point clear let us take a close look at Figs. 2 and 3.

From Fig. 2, and considering only the raw data given for the reference (In-free) GaAs sample, we find that the intensity of the Cr^{2+} ZPL line is about 2 times more important in the epitaxial layer than it was in the corresponding substrate. Asuming all external parameters to have identical values (which is not a bad approximation for intracenter transitions), we end up with a concentration of the (Cr^{2+}-V_{As}) complex 2 times more important in the epitaxial layer than it was in the corresponding substrate. Letting the average distribution of chromium be the same as that of a typical ingot, we would get semi-insulating material. This is just not reflected in the electrical data of Table II. At room temperature, both the numbers of carriers determined by Hall effect measurements and C^{-1} (V) plots are in the range 10^{15} cm^{-3}. This demonstrates (i) that both "optically active" centers investigated in this work do not participate in the compensation of the material (they are both electrically inactive), and (ii) that chromium does not incorporate as efficiently on electrically active positions as it does near a neighboring vacancy (optically active centers).

Concerning the first point, this can be discussed in the light of rather simple theoretical arguments. The point is that, in typical III-V materials, an ideal vacancy with T_d symmetry [simply obtained by removing an anion (cation) from an otherwise perfect lattice] induces twofold and sixfold degenerate levels (including spin) with $a_1(s)$ and $t_2(p)$ symmetry, respectively. For the neutral anion (cation) vacancy there will be three (five) unmatched electrons associated with the bound states of which two lie on the deep $a_1(s)$ state (most of the time they give resonant states with the valence band) and one (three) lie on the $t_2(p)$ orbitals. To summarize, any anion (cation) vacancy leaves antibonding (bonding) p orbitals associated with the four remaining cations (anions) and the corresponding state as a typical donor (acceptor) character. This is best shown in Fig. 11. We display (i) the results of the tight-binding calculations of Talwar and Ting[36] for the

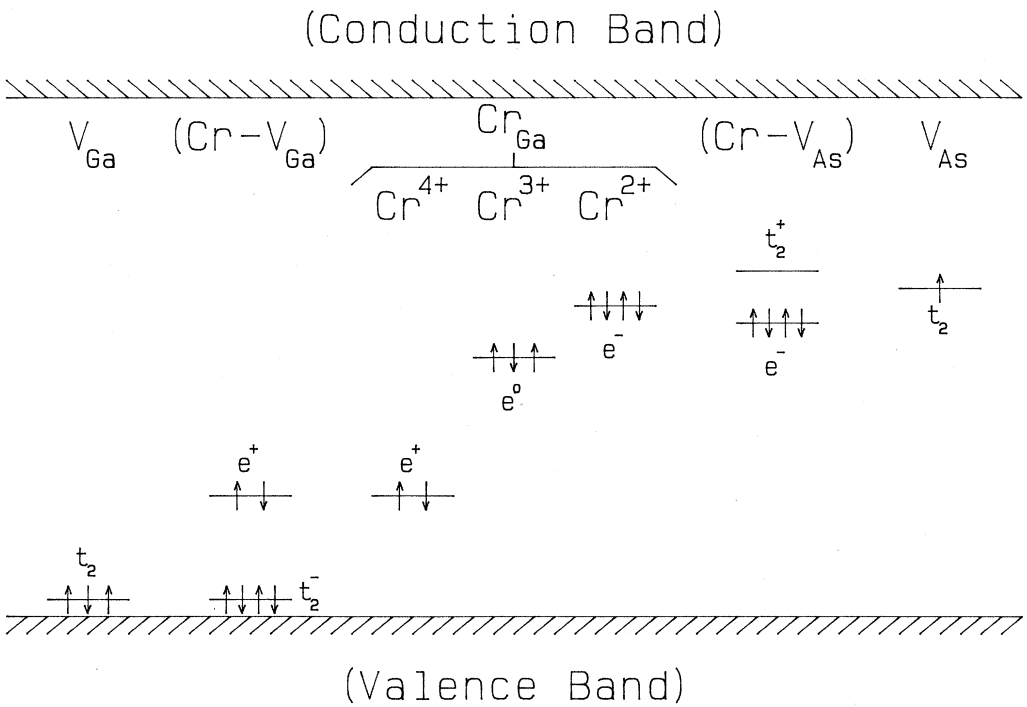

FIG. 11. Schematic energy diagram of the electronic levels associated with (i) isolated vacancies V_{As} and V_{Ga} and (ii) the series of chromium-related centers in GaAs. The triplet states associated with both anion and cation vacancies have been obtained from the work of Talwar and Ting (Ref. 36). The energy position of the e^0-like state of neutral chromium has been adjusted at midgap. The energy differences Cr^{2+}/Cr^{3+} (0.15 eV) and Cr^{3+}/Cr^{4+} (0.4 eV) have been extracted from the molecular cluster calculation of Hemstreet and Dimmock (Ref. 37).

t_2-like states of isolated vacancies in GaAs (V_{Ga} at 0.05 eV and V_{As} at 0.95 eV, respectively, from the top of the valence band) and (ii) the estimated energy positions of the two ionized states of substitutional chromium (Cr^{4+} and Cr^{2+}, respectively). For clarity the neutral Cr^{3+} state of the substitutional impurity (e^0) has been centered at midgap and both energy differences Cr^{2+}/Cr^{3+} (0.15 eV) and Cr^{3+}/Cr^{4+} (0.4 eV) have been obtained from the molecular cluster calculation of Hemstreet and Dimmock.[37] Of course, none of these calculations takes account of lattice relaxation effects and/or electron-electron interaction, so their consideration can only serve illustrative purposes. The point is that, coupling a chromium atom with a neighboring vacancy, one gets in *both* cases a neutral complex: The charge state of chromium, changing from neutral (Cr^{3+}) to ionized (Cr^{2+} or Cr^{4+}, respectively) is able to compensate for the donor or acceptor character of the neighboring vacancy and makes such complexes electrically inactive.

Last, concerning the second point and the mechanism of defect reduction by indium incorporation, we have seen that only chromium-related features (optically active) were drastically removed. This should be discussed more quantitatively in the light of our simple model. We focus now on the DCS which corresponds to a chromium atom at a gallium site, complexed with a neighboring vacancy. Neglecting the presence of the vacancy, and assuming identical probabilities of substitution for all available cationic sites, we would end up with identical results to the one obtained for *EL*2. Clearly, in the range of indium compositions achieved in this work, it would correspond to a very negligible change ($\sim 10^{-3}$) which, of course, does not fit the experimental results. Assuming now a selective incorporation mechanism, and an n-times increased probability for indium to substitute for chromium atoms located near a lattice vacancy, we get an equation similar to Eq. (7),

$$\Delta[\mathrm{Cr}]_{\mathrm{complex}} = -n\frac{[\mathrm{Cr}]_{\mathrm{complex}}}{N_c - [\mathrm{In}]_{\mathrm{Ga}}}\Delta[\mathrm{In}]_{\mathrm{Ga}} , \tag{9}$$

which gives, after straight integration,

$$[\mathrm{Cr}]_{\mathrm{complex}} = [\mathrm{Cr}]^0_{\mathrm{complex}}[1 - nn_i] . \tag{10}$$

Provided n is high enough, this predicts a very fast decrease which follows nicely the experimental data and is illustrated in Fig. 3 for $n \simeq 10^3$ (dashed line). The point is that, after a given indium composition $n_{i,\max}$ (~ 0.1 at. %), most chromium sites associated with a neighboring vacancy have been substituted by indium and this selective mechanism closes down. This is also in agreement with the experimental data: above $n_i = 0.1$ at. %, we find only a standard background. Added to the first contribution, both give the theoretical composition dependence displayed in Fig. 3 (solid line) for $n = 1150$ and demonstrate that, in GaAs:In, there is not necessarily a random incorporation of indium atoms on the gallium sites. In some cases, the isoelectronic dopant *selects* lattice sites close to a point defect (this is the case of chromium complexed with V_{As} or V_{Ga}). Such selective incorporation effects, which involve lattice relaxation effects and a minimization of the crystal total energy, are difficult to deal with theoretically but constitute a key for understanding the physics of defects compensation.

Lastly, we have performed a comparison with bulk GaAs:In,Cr (Refs. 23 and 38) material. We find the following.

(i) In both cases the ZPL shifts toward lower energy versus indium content. Since we are dealing with internal transitions, this is indicative of a change in crystal-field splitting. Based on general crystal-field theory,[39] it was assumed in Ref. 23 that the magnitude of the crystal-field splitting would vary like the fifth power of the lattice constant of the host material. We have checked this point. Figure 12 displays a comparison between the experimental data (solid dots) and a theoretical shift estimated from the standard formula:

$$\Delta E = E_0[(a_{\mathrm{GaAs}}/a_{\mathrm{GaAs:In}})^5 - 1] . \tag{11}$$

Since, on the atomic scale, $Ga_{1-x}In_xAs$ is a very complicated system where all first nearest-neighbor (NN) distances depart from the Vegard law,[40] we have checked relative changes in both the macroscopic (average) lattice constant (dashed line) and the microscopic GaAs NN distance (solid line). Obviously, we find a much better agreement in the latter case which agrees well with the localized nature of this center.

(ii) In both cases, the overall intensity of the chromium-related features decreases versus indium content. However, unexplained discrepancies remain concerning the interpretation of data. In our case we have found a close correlation between the NBE and deep-trap signals (see Fig. 4) but no change in half-width at half maximum (HWHM). On the opposite, in the work of Ref. 23, an increase in HWHM was noticed which ended with a complete disappearance of the structure for indium concentrations in the range 10^{21} cm^{-3}. Such discrepancies should correlate with the different incorporation technique and the different ranges of indium concentration investigated. The probability of finding a perturbing atom in the neighborhood of a complex

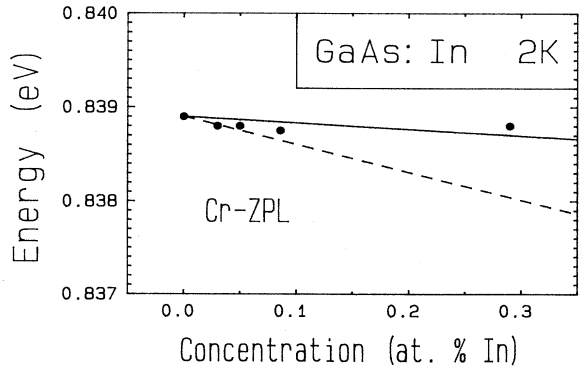

FIG. 12. Composition dependence of the Cr-ZPL energy obtained in this work. Solid and dashed lines are theoretical composition dependences as discussed in the text. The best agreement achieved in the first case demonstrates that the magnitude of the crystal-field splitting in GaInAs varies like the fifth power of the first-nearest-neighbor distancy.

changing from vanishingly small in our case to finite in the case of Ref. 23. In this case it would slightly change (and broaden) the energy levels.

(iii) As already said, when the perturbing (indium) atom comes in a first-neighbor position, this results in the complex (Cr_{Ga}-V_{As}-In_{Ga}) and new Cr-related PL lines (see Sec. III A). In bulk GaAs,[23,25] analyzing both the corresponding intensity and depth profile, evidence was found for pure statistic distributions and in-depth profiles which obey simple diffusion laws. This departs from the results obtained in this work: First, we could not get evidence of the new PL lines and, second, the chromium distribution departs from a standard model.

We could not find in the recent literature any report of In- and Cr-codoped epitaxial samples. However, concerning only In doping, similar investigations have been reported in Ref. 10. They concern liquid phase epitaxy (LPE) and we notice the following.

(i) A decreasing behavior of the deep-level related PL intensity with In content was also noticed. This agrees qualitatively with the results reported in Sec. III.

(ii) The stability observed in this work for $EL2$ contrasts with the strong decrease in DLTS signal reported in Ref. 10. As already said, the DLTS spectra of Ref. 10 were obtained from LPE samples which should be $EL2$-free due to the growth conditions (Ga-rich bath). As a consequence, this DLTS signal, sensitive to indium incorporation, is certainly not $EL2$ related. On the other hand, slight reductions in $EL2$ density (in a ratio of typically 3:5) have been reported in bulk dislocation-free GaAs:In (Refs. 1, 2, and 5) and agree better with the results reported in this work. The close correlation between $EL2$ and the dislocation density reduction is still under discussion[4,32,33,41,42] and, in this context, the $EL2$ stability observed in our samples confirms the results of Refs. 41 and 42. It indicates that there is no significant correlation between the concentration of arsenic antisites and the indium content.

VI. CONCLUSION

Concerning the specific role of indium in both the decay of our deep-level related PL signals and the increase in the NBE intensity, the following conclusions can be drawn.

(i) Concerning normal cationic sites, indium incorporates like a standard constituent of the solid solution $Ga_{1-x}In_xAs$.

(ii) Concerning simple point defects (shallow impurities) differences exist between impurities which incorporate on the cationic sites (Zn and Mg), on the one hand, and impurities which incorporate on the anionic sites (C), on the other hand. Such differences rely on microscopic effects.

(iii) Concerning more complex defects, which involve the association of impurities with vacancies or antisites, we find a behavior which *depends on the defect investigated.* Both concentrations of (Cr-V_{As}) and (Cr-V_{Ga}) exhibit a drastic decrease versus indium concentration while $EL2$ appears mainly insensitive. Indium does not reduce the concentration of gallium vacancies: It acts only in the field of the vacancies. This is the reason why the concentration of Cr-related centers has been so drastically reduced. Both atomic species would incorporate preferentially on the same sites and indium does it faster.

None of these results are in agreement with the standard views which have long being dominating the literature. Indeed, concerning the role of indium in the decay of the deep-level related PL signals, one generally assumes (1) substitutional indium atoms occupy Ga sites and directly reduce the concentration of Ga vacancies. Therefore the probability of formation of *all* related V_{Ga} defects (including the contamination by substitutional Cr_{Ga}) would be reduced and the probability of formation of the (D-V_{Ga}) complex would be even more. We have found that the concentration of V_{Ga} remains constant and that only the chromium concentration seems to vary. This discards this simplistic viewpoint.

(2) As suggested in Ref. 10, most of the impurities observed in the main PL bands involve an outdiffusion process from the substrate to the epitaxial layers. This process could be sometimes blocked by the strain associated with the lattice mismatch (at the interface[43] or in the epitaxial layer[10]). In our case the dominant impurity was chromium. We have found that, apart from the standard diffusion mechanism through the interface, it was an effect of chromium incorporation through the gas phase, and, because of a higher incorporation rate of indium near lattice point defects, this second source was selectively blocked. This is the real source of indium-related effects in our series of OMVPE samples.

ACKNOWLEDGMENTS

One of the authors, J. P. Laurenti, is especially grateful to the Deutscher Akademischer Austauschdienst (DAAD) for financial support of his visit in Institute of Semiconductor Electronics (Aachen, Federal Republic of Germany). This work was also supported in part by the French-German Scientific Cooperation Program (PROCOPE).

*Permanent address: Groupe d'Etudes des Semiconducteurs, Institut de Recherche sur les Matériaux pour l'Electronique, Université des Sciences et Techniques du Languedoc, F-34060 Montpellier CEDEX, France.

[1]G. Jacob, M. Duseaux, J. P. Farges, M. B. Van den Boom, and P. J. Roksnoer, J. Cryst. Growth **61**, 417 (1983).

[2]M. Duseaux and S. Martin, in *Semi-Insulating III-V Materials, Kah-nee-ta, 1984,* edited by D. C. Look and J. S. Blakemore (Shiva, Nantwich, U.K., 1984), p. 118.

[3]S. McGuigan, R. M. Thomas, D. L. Barrett, H. M. Hobgood, and B. W. Swanson, Appl. Phys. Lett. **48**, 1377 (1986); also see H. M. Hobgood, S. McGuigan, J. A. Spitznagel, and R.

N. Thomas, *ibid.* **48**, 1654 (1986).
[4]For a recent review, see J. P. Fillard, Ann. Télécommun. **42**, 149 (1987).
[5]H. Kimura, C. B. Afable, H. M. Olsen, A. T. Hunter, K. T. Miller, and H. V. Winston, in *Proceedings of the Extended Abstracts of the 16th Conference on Solid State Devices and Materials, Kobe, 1984* (Japan Business Center for Academic Societies, Tokyo, 1984), p. 59.
[6]B. Pichaud, N. Burle-Durbec, and F. Minari, J. Cryst. Growth **71**, 648 (1985).
[7]N. Noto, Y. Kitagawara, T. Takahashi, and T. Takenaka, Jpn. J. Appl. Phys. **25**, L394 (1986).
[8]Y. Fujiwara, Y. Kita, Y. Tonami, T. Nishino, and Y. Hamakawa, Appl. Phys. Lett. **49**, 161 (1986).
[9]H. Ehrenreich and J. P. Hirth, Appl. Phys. Lett. **46**, 668 (1985).
[10]H. Beneking, P. Narozny, and N. Emeis, Appl. Phys. Lett. **47**, 828 (1985).
[11]P. Narozny and H. Beneking, Electron. Lett. **21**, 1050 (1985).
[12]H. Takeuchi, M. Shimohara, and K. Oe, Jpn. J. Appl. Phys. **25**, L303 (1986).
[13]P. L. Gourley, T. J. Drummond, and B. L. Doyle, Appl. Phys. Lett. **49**, 1101 (1986). See also G. C. Osbourn, P. L. Gourley, J. J. Fritx, R. M. Biefiels, R. L. Dawson, and T. E. Zipperiam, in *Semiconductors and Semimetals,* edited by R. K. Willardson and A. C. Beer (Academic, New York, in press), and references therein.
[14]J. P. Laurenti, P. Roentgen, K. Wolter, K. Seibert, H. Kurz, and J. Camassel, Phys. Rev. B **37**, 4155 (1988).
[15]See, for instance, B. Gil, J. P. Albert, J. Camassel, H. Mathieu, and C. Benoit à la Guillaume, Phys. Rev. B **33**, 2701 (1986), and references therein.
[16]H. Mariette, Y. Marfaing, and J. Camassel, in *Proceedings of the 18th International Conference on the Physics of Semiconductors, Stockholm, 1986,* edited by O. Engström (World Scientific, Singapore), p. 1405.
[17]H. J. von Bardeleben, D. Stievenard, and J. C. Bourgoin, Appl. Phys. Lett. **47**, 970 (1985); also see B. K. Meyer, D. M. Hofmann, J. R. Niklas, and J. M Spaeth, Phys. Rev. B **36**, 1332 (1987).
[18]K. A. Brauchle, D. Bimberg, K. H. Goetz, H. Jürgensen, and J. Selders, Physica **129B**, 426 (1985).
[19]C. A. Bates and K. W. Stevens, Rep. Prog. Phys. **49**, 783 (1986).
[20]M. S. Skolnick, M. R. Brozel, and B. Tuck, Solid State Commun. **43**, 379 (1982).
[21]J. Barrau, Do Xuan Thann, M. Brousseau, J. C. Brabant, and F. Voillot, Solid State Commun. **44**, 395 (1982).
[22]B. Devaux, B. Lambert, and G. Picoli, J. Appl. Phys. **55**, 4356 (1984), also see Y. Fujiwara, Y. Kita, Y. Tonami, T. Nishino, and Y. Hamakawa, Jpn. J. Appl. Phys. **24**, 1479 (1985); J. Phys. Soc. Jpn. **55**, 3741 (1986).
[23]Y. Fujiwara, Y. Kita, Y. Tonami, T. Nishino, and Y. Hamakawa, Appl. Phys. Lett. **49**, 161 (1986); Jpn. J. Appl. Phys. **25**, L232 (1986).
[24]B. Tuck, G. A. Adegboyega, P. R. Jay, and M. J. Cardwell, Inst. Phys. Conf. Ser. **45**, 114 (1979), also see J. Kasahara and N. Watanabe, Jpn. J. Appl. Phys. **19**, L151 (1980).
[25]K. H. Goetz, D. Bimberg, K. A. Brauchle, H. Jürgensen, J. Selders, M. Razeghi, and E. Kuphal, Appl. Phys. Lett. **46**, 277 (1985).
[26]E. W. Williams, Phys. Rev. **168**, 922 (1968).
[27]L. Samuelson, P. Omling, H. Titze, and H. G. Grimmeiss, J. Cryst. Growth **55**, 164 (1981); also see C. J. Hwang, J. Appl. Phys. **40**, 4584 (1969), and references therein.
[28]J. S. Blakemore, S. G. Johnson, and S. Rahimi, in *Semi-Insulating III-V Materials, Evian, 1982,* edited by S. Markram-Ebeid and B. Tuck (Shiva, Nantwich, U.K., 1982), p. 172.
[29]G. H. Stauss, J. J. Krebs, S. M. Lee, and E. M. Zwiggard, Phys. Rev. B **22**, 3141 (1980).
[30]D. C. Look, S. Chaudhuri, and L. Eaves, Phys. Rev. Lett. **49**, 1728 (1982).
[31]L. M. R. Scolfaro, R. Pintanel, V. M. S. Gomes, J. R. Leite, and A. S. Chaves, Phys. Rev. B **34**, 7135 (1986).
[32]M. Tajima, Appl. Phys. Lett. **46**, 484 (1985); also see M. Tajima, A. Yakata, T. Kikuta, N. Tsukada, and K. Ishida, in *Semi-Insulating III-V Materials, Hakone, 1986,* edited by H. Kukimoto and S. Miyazawa (North-Holland, Amsterdam, 1986), p. 305.
[33]E. R. Weber and P. Omling, in *Festkörperprobleme (Advances in Solid States Physics),* edited by P. Grosse (Vieweg, Braunschweig), Vol. XXV, p. 623, and references therein; also see S. Miyazawa, in Ref. 32, p. 3.
[34]M. O. Watanabe, A. Tanaka, T. Udagawa, T. Nakanisi, and Y. Zohta, Jpn. J. Appl. Phys. **22**, 923 (1983).
[35]H. Z. Zhu, Y. Adachi, and T. Ikoma, J. Cryst. Growth **55**, 154 (1981).
[36]D. N. Talwar and C. S. Ting, Phys. Rev. B **25**, 2660 (1982).
[37]L. A. Hemstreet and J. O. Dimmock, Phys. Rev. B **20**, 1527 (1979).
[38]Y. Fujiwara, Y. Kita, Y. Tomami, T. Nishino, and Y. Hamakawa, in Ref. 32, p. 115.
[39]S. Sugano, Y. Tanabe, and H. Kamimura, *Multiplets of Transition-Metal Ions in Crystals* (Academic, NY, 1970), p. 14.
[40]J. C. Mikkelsen, Jr. and J B. Boyce, Phys. Rev. B **28**, 7130 (1983).
[41]J. Bittebierre, R. T. Cox and E. Molva, in *Proceedings of the 14th International Conference on Defects in Semiconductors,* Paris, 1986, Vols. 10–12 of Materials Science Forum, edited by H. J. von Bardeleben (Trans Tech, Aedermannsdorf, 1986), p. 365.
[42]J. P. Fillard, P. Gall, M. Asgarinia, M. Castagne, and M. Baroudi, Jpn. J. Appl. Phys. **27**, L899 (1988).
[43]J. H. van der Merwe, J. Appl. Phys. **41**, 4725 (1970).